

Estimating unconfined compressive strength of unsaturated cemented soils using alternative evolutionary approaches

Navid Kardani^a, Annan Zhou^{a,*}, Shui-Long Shen^b, Majidreza Nazem^a

^a Civil and Infrastructure Engineering Discipline, School of Engineering, Royal Melbourne Institute of Technology (RMIT), Victoria 3001, Australia

^b Department of Civil and Environmental Engineering, College of Engineering, Shantou University, Shantou, Guangdong 515063, China

ARTICLE INFO

Keywords:

Unsaturated cemented soils
Unconfined compressive strength
Artificial neural network
Evolutionary optimisation
Parametric analysis

ABSTRACT

The use of cement as a curing agent has been widely adopted in soft soil engineering to increase the strength of soft soil. The cemented soil is gradually exposed to the air and in a natural environment becomes unsaturated. Unconfined compressive strength (UCS) of the unsaturated cemented soils is a key parameter for assessing their strength behaviour. UCS determination of unsaturated cemented soils by using laboratory methods is a complex, time-consuming, and expensive procedure due to the difficulty in suction control. This study aims to model the UCS of unsaturated cemented Wenzhou clay, i.e., capture the nonlinear relations between UCS and its influential variables including cement content (%), dry density (g/cm^3) and suction (MPa) for the first time by using machine learning approach. Toward this aim, three advanced computational frameworks are developed based on hybrid evolutionary approaches in which evolutionary optimisation algorithms including genetic algorithm (GA), particle swarm optimisation (PSO) and imperialist competitive algorithm (ICA) are hybridised with artificial neural network (ANN). Results show that developed models have a great ability to mimic the nonlinear relationships between UCS and its influential variables and PSO-ANN presents the best performance among three models on the training dataset with $R^2 = 0.9888$, $RMSE = 0.129$ and $VAF = 97.742$, and testing dataset with $R^2 = 0.9412$, $RMSE = 0.237$ and $VAF = 90.414$. To facilitate engineering application, an engineering database for Wenzhou soft clay at different cement ratios (up to 11%), suctions (up to 300 MPa) and dry densities ($1\text{--}1.5 \text{ g}/\text{cm}^3$) is built by using the developed PSO-ANN model.

Introduction

Soft soils are mostly along coastal areas with high ground water level; however, they can also be partially saturated due to excavation, dewatering, compaction, stabilisation, and biogas. The features of soft soils include low bearing capacity, high compressibility and low shear strength. Soil stabilisation is a modification technique for improving soil behaviour under applied loads. In recent years various soil enhancement methods have been used, which are divided into mechanical and chemical categories [1]. The most popular mechanical method is soil reinforcement, while chemical additives are also being used as an alternative method for soil enhancement. In many situations, chemical enhancement is preferred to mechanical method, where chemical reactions play a primary role. Lime and cement are two useful traditional chemical additives for soil stabilisation [2].

Employing cementitious materials to enhance the stiffness, stability

and bearing capacity of soils is one of the most popular methods for modifying the properties of soft soils. Among the available chemical additives, the widely used additive for this purpose is ordinary Portland cement (OPC) due to its availability and cost [3]. As a composite material, which is formed by curing and compaction, compacted cemented soil is usually considered in an unsaturated state [4,5]. Moisture content, soil properties, type of cement, cement content, temperature, curing age, mixing method and stress history are some of the influential factors in the strength of cemented soil [6–8]. With considering cemented soils as unsaturated soils in most of the cases, it is important to consider suction and dry density as influential variables [9] to determine the unconfined compressive strength (UCS) of cemented soils.

However, during laboratory tests, to achieve target suctions, suction equilibrium can only be achieved by a long time, particularly when vapour equilibrium technique (VET) is adopted to realise a wide range of suction up to 287 MPa [10]. For each sample, the equilibrium time by

* Corresponding author.

E-mail addresses: navid.kardani@rmit.edu.au (N. Kardani), annan.zhou@rmit.edu.au (A. Zhou), shensl@stu.edu.cn (S.-L. Shen), Majidreza.nazem@rmit.edu.au (M. Nazem).

using VET method is longer than 4 weeks with a strict temperature control. When various dry density and cement contents apply, the testing time can be very huge. In addition, the suction controlled by VET is dependent on the type of the salt solutions. Eight different saline solutions (i.e., K_2SO_4 , KCl, NaCl, KI, K_2CO_3 , $MgCl_2 \cdot 6H_2O$, CH_3COOK , and LiCl) are commonly used to achieve suction range from 3.29 MPa to 286.70 MPa. For example, the suction corresponding to saturated LiCl solution at 20 °C is 286.70 MPa and suction to saturated CH_3COOK is 198.14 MPa. However, the suction between 286.70 MPa and 198.14 MPa cannot be achieved due to lack of corresponding saline solutions. Therefore, UCS of unsaturated cemented soil with suction between 286.70 MPa and 198.14 MPa cannot be measured easily. Therefore, measuring the UCS of unsaturated cemented soil is challenging and time-consuming.

In the recent decades, intelligent approaches such as machine learning (ML) algorithms have been widely used in geotechnical engineering and soil mechanics including, but not limited to, soil classification [11], soil liquefaction [12,13], jet grouting [14], dynamic behaviour of soils [15], slope stability [16,17], and bearing capacity of piles [18,19]. More specifically, regarding the reproducing strength behaviour of geomaterial like UCS, Javdanian and Lee [20] presented a study on the evaluation of UCS of the geopolymmer stabilised cohesive soils using group method of data handling (GMDH). They considered composition of the geopolymers and soil characteristics as influential variables. Das et al. [21] used artificial neural network (ANN) and support vector machine (SVM) to estimate the UCS of the stabilised soil. Liquid limit, plasticity index, clay fraction, sand, gravel, moisture content and cement content were considered as input variables of the models. Ghorbani and Hasanzadehshoili [22] employed ANN and evolutionary polynomial regression (EPR) to estimate UCS and California bearing ration (CBR) of micro silica-lime stabilised sulphate silty sand through its composition.

As evidenced above, various studies have been performed to evaluate the predictive performance of intelligent approaches on UCS of soils. However, the UCS of unsaturated cemented soils has not been studied by using machine learning approaches. Considering the challenges above mentioned in testing unsaturated cemented soils, powerful machine learning tools that can predict the UCS of unsaturated cemented soils at various suctions, cement contents, and dry densities based on limited number of tests are very demanding. On the other hand, in terms of advances in applying machine learning techniques for geomaterial behaviour, application of hybrid evolutionary approaches has never been studied in predicting the UCS and the feasibility of these methods have not been thoroughly investigated. Numerous studies in the field of science and engineering have been conducted to boost the efficiency of traditional ML algorithms, such as ANN [23–25]. While traditional ML algorithms deliver better results in comparison to statistical techniques, instead of finding the precise global minima, they are more likely to be caught up in local minima, which in turn generates unwanted results. Researchers are therefore now adopting optimisation algorithms (OAs) to update the learning parameters of classical ML algorithms to mitigate this problem, which in turn would lead to achieving notable outcomes [26–30]. In addition, there is a vital need to tune the parameters of optimisation algorithms properly before implementing them on the datasets, while the capability of parameter optimisation has not been fully explored on UCS of unsaturated cemented soils dataset, which also requests a systematic, comprehensive comparative study of hybrid evolutionary approaches.

By a comparative manner, this study implements three advanced computational frameworks based on hybrid evolutionary approaches to tackle the research gap in the literature regarding reproduction of the UCS of unsaturated cemented soils. These three frameworks consist of hybridisation of imperialist competitive algorithm (ICA) and artificial neural networks (ANN), i.e., ICA-ANN, hybridisation of genetic algorithm (GA) and ANN, i.e., GA-ANN, and hybridisation of particle swarm optimisation (PSO) and ANN, i.e., PSO-ANN. In this study, a dataset

based on the experimental study on Wenzhou clay by authors [3] which consists of 96 samples, is used for training and testing. Cement content, dry density, and suction are the input parameters of the models and UCS of the unsaturated cemented soils is the output of the model. Root mean square error (RMSE), R-squared value (R^2) and variance accounted for (VAF) are used as performance measures to evaluate and compare the performance of three advanced computational frameworks. Finally, to facilitate engineering application, an engineering database for Wenzhou soft clay at different cement ratios (up to 11%), suctions (up to 300 MPa) and dry densities (1–1.5 g/cm³) is built by using the developed hybrid evolutionary approaches.

Significance of the subject

Cement has been frequently used as a curing agent in soft soil engineering to increase the strength of soft soil. In a natural environment, the cemented soil is progressively exposed to the air and becomes unsaturated. The unsaturated cemented soils' unconfined compressive strength (UCS) is an important measure for determining their strength behaviour. Due to the difficulty in suction control, determining the UCS of unsaturated cemented soils using laboratory methods is a complex, time-consuming, and expensive task. In this regard, Computational intelligence approaches including hybrid machine learning models, with their non-linear modelling capabilities, are becoming an excellent source of predictive tools delivering solutions to ever-increasingly complicated optimisation issues. Despite the good performance, a conventional ML method such as ANN has its own limitations, arguably, the black-box nature, high computational cost and overfitting issue outdoes the model's simplicity and hence they are not capable enough in generating the practical prediction in the validation phase [31–33]. As a result, to tackle the drawbacks of traditional machine learning (ML) techniques, researchers are now employing metaheuristic optimization techniques to improve the generalization capabilities of traditional ML techniques [34–39]. This paper presents an advanced application of evolutionary based ANN algorithms including ICA, GA and PSO-based ANN for the estimation of UCS of unsaturated cemented soils. The results of this work will provide engineers with tools to predict UCS of unsaturated cemented soils.

Methodology

As illustrated in Fig. 1, in this study, three advanced computational frameworks are developed to predict the nonlinear relationships between UCS of unsaturated cemented soil and its influencing variables. First, the data is divided into training and testing datasets and then the hybridisation process is started where each evolutionary algorithm is used to optimise the weights and biases of the ANN in an optimisation process in order to enhance the learning stage of the ANN using training dataset. Then, the trained hybrid models are applied on the testing dataset to evaluate and compare the modelling results. In this section, details of the evolutionary algorithms as well as hybridisation with ANN are explained.

Imperialist competitive algorithm

Imperialist competitive algorithm (ICA) is considered as a relatively new strategy for optimisation based on socio-political evolution of human beings or social Darwinism. ICA was first introduced by Atashpaz-Gargari and Lucas [40] and was used in global optimisation problems. ICA is a robust computational evolutionary algorithm which is based on imperialist competitive through governmental power and policy systems [41]. Like other evolutionary algorithms, ICA also starts with a random initialisation of the population. In ICA population is called countries (number of countries: N_{cou}) and is categorised into colonies (number of colonies: N_{col}) and imperialists (number of imperialists: N_{imp}) based on their cost functions, where countries with lower

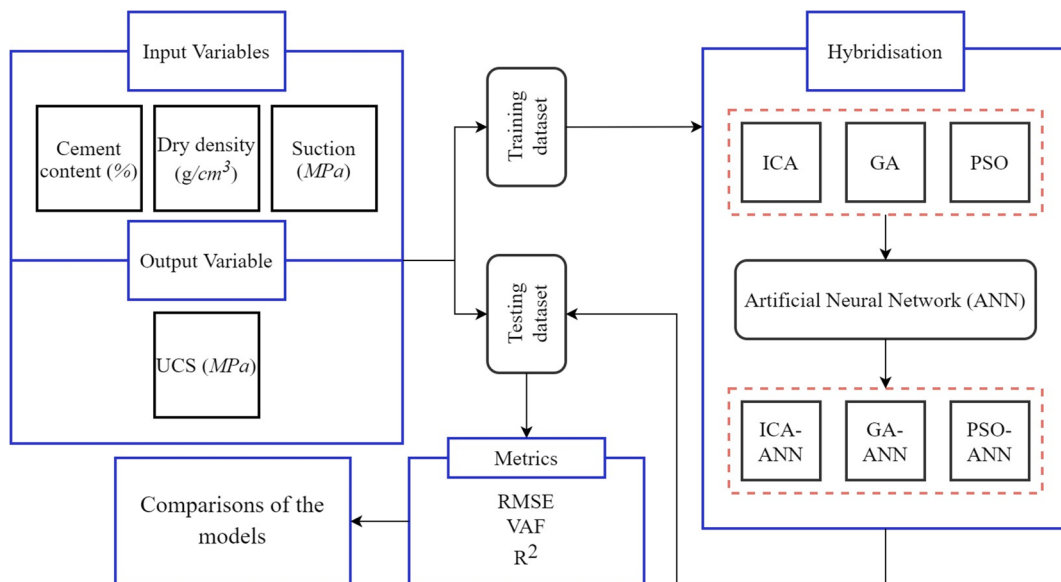


Fig. 1. Methodology of this study.

cost functions are assigned as imperialist and the rest of the countries are assigned as colonies. The empires are established by the distribution of colonies, based on imperialist initial power, between the imperialist countries [42]. An imperialist's normalised cost can be achieved through:

$$C_n = c_n - \max_i \{c_i\} \quad (1)$$

where C_n stands for normalised cost of n^{th} imperialist, c_n shows the cost of n^{th} imperialist. Based on Eq. 1, normalised power of an imperialist can be calculated using Eq. 2 as below:

$$P_n = \left| \frac{C_n}{\sum_{i=1}^{N_{imp}} C_i} \right| \quad (2)$$

Accordingly, the initial N_{col} for n^{th} imperialist can be determined as:

$$N.C_n = \text{round}\{P_n \cdot N_{col}\} \quad (3)$$

where $N.C_n$ stands for the number for the n^{th} imperialist. This is how the colonies are split between empires. The second step is called assimilation where the colonies run distance of x toward their imperialists and x is a uniform random number:

$$x \sim U(0, \beta \times d) \quad (4)$$

where d is the distance between a colony and its imperialist and β is a number greater than 1 and close to 2. Another parameter (deviation θ) which is a uniform random number is used to increase the search space.

$$\theta \ U(-\gamma, \gamma) \quad (5)$$

where γ is an arbitrary parameter. In this study, γ and β are considered as $\frac{\pi}{4}$ and 2, respectively as they lead to better results. Two further steps are (1) revolution, where some of the colonies run suddenly through a new random position to prevent local optima trapping, and (2) swapping a colony with its imperialist, where the colony finds the lower cost function position than its imperialist. Then, we calculate the total power of an empire:

$$T.C_n = Cost(imperialist_n) + \xi \text{ mean } \{Cost(coloneis \text{ of } empire_n)\} \quad (6)$$

where $T.C_n$ is a small positive number close to zero which stands for total cost of n^{th} empire. ξ is considered to be 0.1. Through the process of possessing colonies by imperialists, some empires may collapse due to

losing all their colonies, which is known as imperialist competition. Imperialist competition can be modelled as follows:

$$N.T.C_n = T.C_n - \max_i\{T.C_i\} \quad (7)$$

$$P_{pn} = \left| \frac{N.T.C_n}{\sum_{i=1}^{N_{imp}} N.T.C_i} \right| \quad (8)$$

where $N.T.C_n$ stands for normalised total cost of n^{th} empire and P_{Pn} is the probability of possession of weakest imperialist. The weakest empire is eliminated during the imperialist competition when all its colonies are possessed by other stronger empires. In this study, revolution rate, assimilation coefficient and assimilation angle coefficient are considered to be 0.3, 2 and 0.5, respectively [40].

Genetic algorithm

Genetic algorithm (GA) is considered as a mathematical expression of the natural-biological evolution of human beings. GA, first put forth by John Holland [43], has been used in different applications and resulted in outstanding outcomes. In GA, the correct responses of a generation are combined in order to attain the optimal solution, based on the theory of survival of the fittest in living organisms [44]. In each step, chromosomes which are the counterparts of the countries in ICA, are randomly selected from the current populations (parents) and used to produce the next generation.

Toward this aim, three main types of genetic operators including selection operator, crossover operator and mutation operator are used in each step. Selection operator selects a member of a generation which is supposed to participate in the reproduction process based on the fitness criteria. The better the chromosome fits, the more likely it will be selected. Crossover operator (see Fig. 2) selects a locus between two chromosomes at random to create offspring. Crossover leads to generate new solutions stochastically based on an existing population. The crossover point is randomly selected in the range of 1 and $\min(LA^{P_1}, LA^{P_2}) - 1$, where LA^{P_1} and LA^{P_2} are the number of location areas in parent solution P_1 and P_2 . Mutation operator (see Fig. 2) randomly re-permutes (flips) the sequence of the bits in chromosomes, in a way that the topology is not changed but different placements is generated [45]. In this study, recombination, crossover and mutation are considered to be 0.15, 0.5 and 0.35, respectively [46].

The steps through GA are as follows:

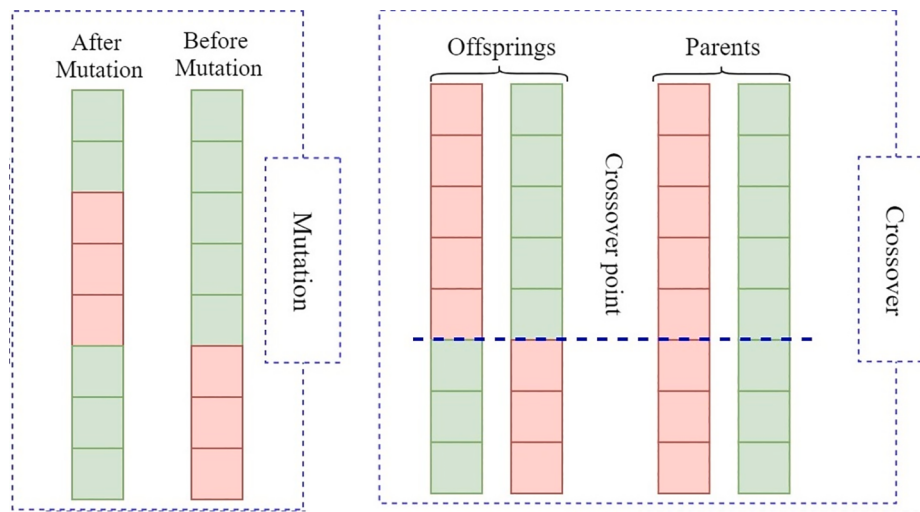


Fig. 2. Schematic of crossover and mutation rules.

Step 1: Initialize the random population of n chromosomes, i.e., potential solutions of the problem.

Step 2: Compute the fitness of each chromosome in the population.

Step 3: Execute and repeat following steps until the creation of n offspring:

- (1) Choose a pair of chromosomes that play parents' role. The probability of a selected individual is typically a function of fitness.
- (2) Crossover the pair at a randomly selected point based on a probability to form two offspring. If there is no crossover, generate two offspring, which are exact copies of their respective parents.
- (3) Mutate the two offspring based on probability (the rate of mutation) at each locus and position the resulting chromosomes in the new population.

Step 4: Replace the existing population with the new population.

Step 5: If the stopping criterion is not met, go to step 2. Otherwise, deliver the best solution.

Particle swarm optimisation algorithm

Particle swarm optimisation (PSO) was proposed by Eberhart and Kennedy [47]. PSO is a population-based optimisation method which is inspired by the birds flocking patterns in order to obtain promising position (precise objectives) within a multidimensional space. Like evolutionary algorithms, searches are performed by the PSO algorithm utilising a swarm of particles which are updated in each iteration (see Fig. 3). Each particle alters its direction in the problem space in order to find the optimum position based on its personal best position (P_b), the global best position (i.e. best experience of all other members, P_g) and its velocity [48]. During the optimisation, particles not only strive to obtain the best P_b , but change their direction towards the P_g . In the meantime, the velocity of a particle is updated based on the difference between P_g and P_b .

$$V_i^{t+1} = \omega V_i^t + c_1 r_1^t (P_i^t - X_i^t) + c_2 r_2^t (P_g^t - X_i^t) \quad (9)$$

$$X_i^{t+1} = X_i^t + V_i^{t+1} \quad (10)$$

where velocity is shown by V , r_1 and r_2 are random numbers in the range of $[0,1]$, P shows the best position while personal and global are shown by subscripts i and g , respectively. Trust parameters, which denote the confidence level of the particle toward its own position and swarm position, are shown by c_1 and c_2 which both have the value of 2 in this study. ω represents inertia weight. The decreasing of inertia weight

along with the time is shown by:

$$\omega^t = \omega_{\max} - \frac{\omega_{\max} - \omega_{\min}}{t_{\max}} t \quad (11)$$

where ω_{\max} and ω_{\min} stand for final and primary inertia weight values, respectively. Suitable values for ω_{\min} and ω_{\max} are 0.4 and 0.9, respectively. t_{\max} is in accordance with a maximum number of iterations [49].

Hybridisation of optimisation algorithms and artificial neural network model

The recent technical and programming developments have led to the implementation of different approaches to artificial intelligence [50,51]. ANN is among prominent smart approaches employed as a global approximator to analyse regression and classification problems [52]. ANN consists of three types of layers including input, hidden and output layers. Neurons in the input layer whose numbers are the same as input variables of the problem, receive the data. The signal then goes through the hidden layers where the analysis is carried out using weights (W) and biases (b). Mathematical wise, the signal from inputs is first multiplied by the weights and then bias vector is added to the signal. Then the adapted signal goes under activation function through activating process. In this study Tangent-sigmoid function ($Tansig(x) = \frac{2}{1-e^{-2x}} - 1$) is used for the activation process. This process continues to the last hidden layer and lastly the output is released from the output layer which has the same number of nodes as in the output of problem. The optimum topology of the ANN is determined in a trial-and-error process to be 3-10-1 which means 3 neurons in input layer, 10 neurons in the hidden layer and 1 neuron in output layer. Optimising the values of weights and biases in ANN algorithms is the crucial task to obtain accurate result. For this purpose, in this study three evolutionary optimisation algorithms are hybridised with ANN to attain the optimum values of W and b (Fig. 4). Recent years have seen a considerable increase in applying hybrid evolutionary models to different areas of engineering. For example, here are some studies on using ICA-ANN [53–55], GA-ANN [56–58] and PSO-ANN [59–61] for engineering applications.

Data description and performance metrics

In this research, three hybrid evolutionary models are applied to the dataset of 96 cases of unsaturated cemented soil to predict the UCS through a comparative study. Dataset from Yu et al. (2019) is employed here (see Appendix A). The soft clay used in Yu et al. [3] was collected from a construction site in Wenzhou. The moisture content of soft clay is

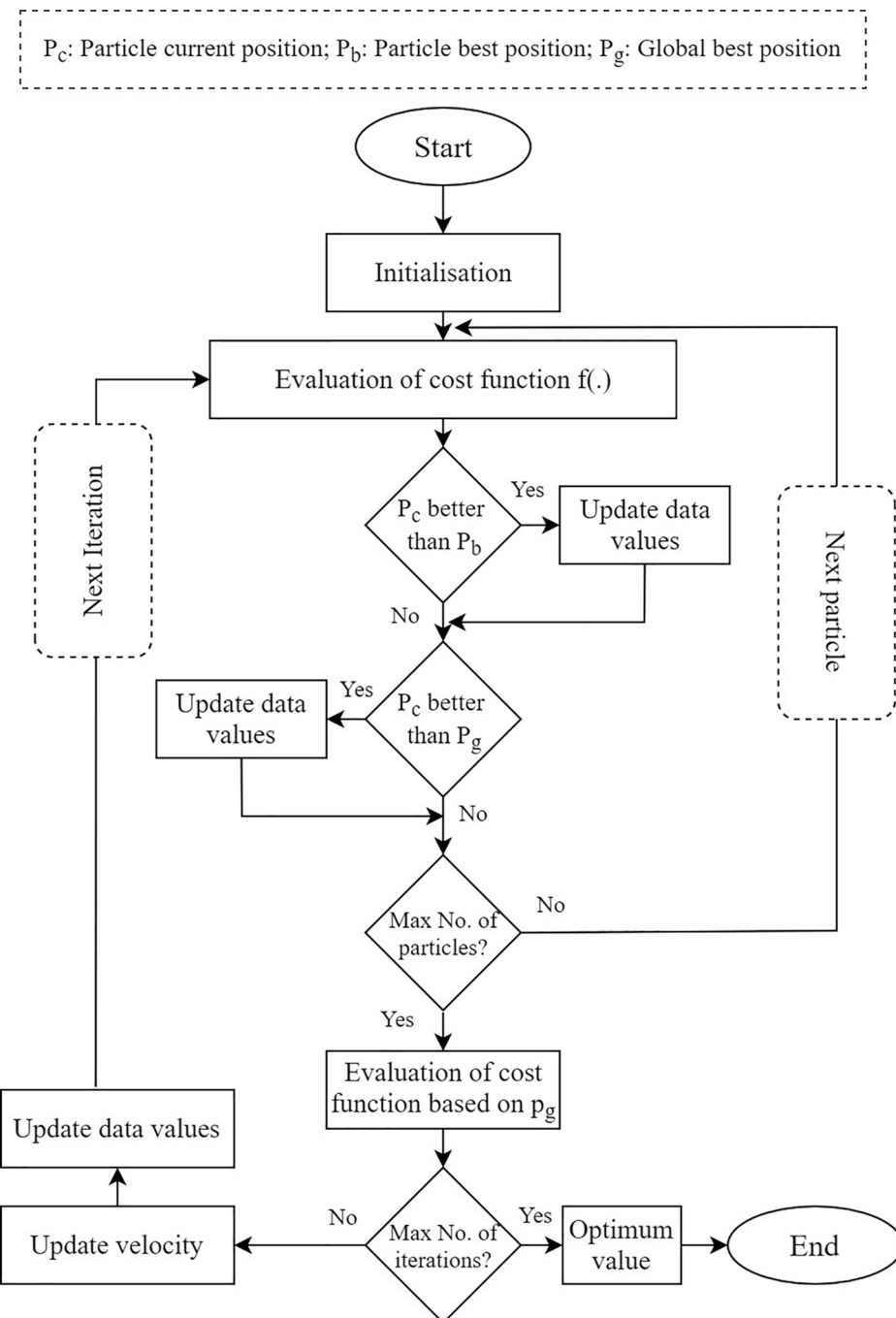


Fig. 3. General Flowchart of PSO algorithm.

74.5% in the field. Prior to the test, the field soil was dried in oven, crushed and passed through a 2 mm sieve. The cement was PO42.5R Portland cement, manufactured by a commercial cement company. In this study, we use three influential variables including cement content (%), dry density (g/cm^3) and suction (MPa). Table 1 shows the statistical summary of the input and output variables, while Fig. 5 illustrates the correlation matrix of the dataset which indicate the correlation coefficients between variables and presents the nonlinear relationships between UCS and its influential variables.

In this study, firstly, to maintain the generalisation capability of the hybrid models and control the over-fitting and under-fitting problems, the dataset is split into training dataset and testing dataset with the ratio of 7–3. It means that 70% of the cases are assigned to the training dataset and 30% of the cases are included in the testing dataset based on the

random selection. Secondly, the dataset is normalised prior to modeling, to change the values of all variables to a common scale without distorting differences in the range of values. As shown in Fig. 6, box plots are used to demonstrate the input data distribution through minimum, first quartile, median, third quartile and maximum values for each influential variable. It is shown that suction has the widest range of values, while cement content and dry density have 4 and 3 values, respectively. Some outliers can be seen for the variables which display the values out of the maximum of 1.5 inter quartile range (IQR).

Fig. 7 shows that the distribution of unconfined compressive strength (UCS) of unsaturated cemented soil is skewed right. On the right side, there are a few data points with UCS values higher than the rest. Most of the data points are between 0.1 and 10 (MPa) and a few cases are between 10 and 20 (MPa). Few cases show 20 (MPa) or higher. The

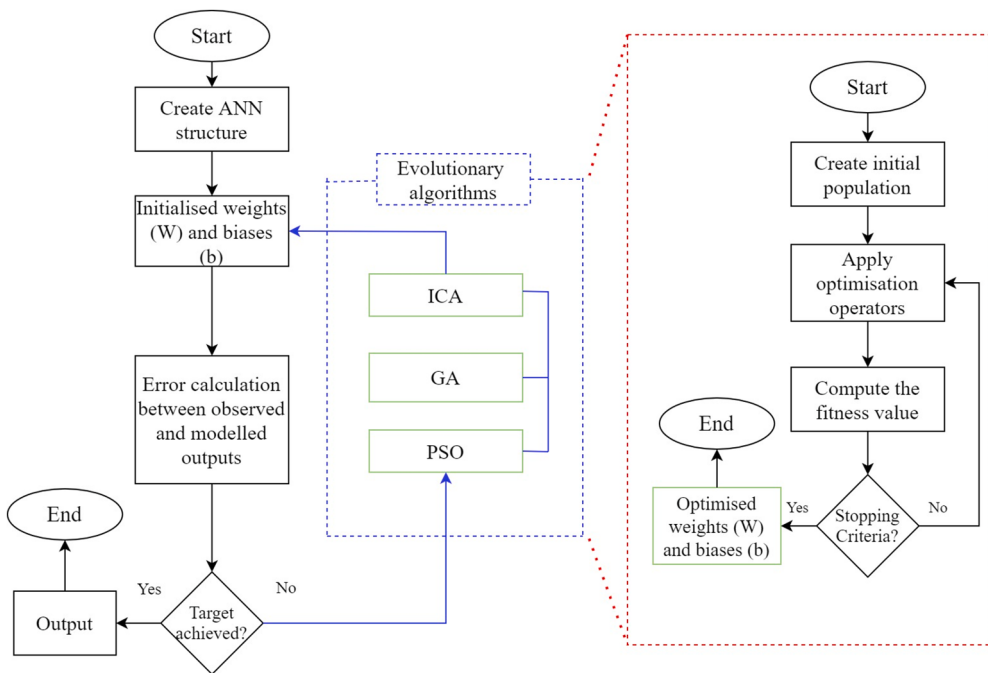


Fig. 4. Hybridisation of ANN and evolutionary algorithms.

Table 1
Summary of the dataset (count = 96).

Variable	Mean	Standard deviation	Minimum	Maximum
Cement content (%)	4.0	2.93	0.0	8.0
Dry density (g/cm ³)	1.23	0.12	1.08	1.38
Suction (MPa)	107.42	93.12	3.29	286.7
UCS (MPa)	3.57	4.1	0.102	22.05

skewness value for this figure is 2.218.

In this paper, root mean squared error (RMSE), R-squared (R^2) and variance accounted for (VAF) are used between observed values and modelled values of UCS to indicate the modelling potential of proposed models. R-squared as a statistical metric is used to show the performance of the model in approximating the real data points. $R^2 = 1 - \frac{\sum_{i=1}^N (y_i^o - y_i^m)^2}{\sum_{i=1}^N (y_i^o - \bar{y}^o)^2}$, where y_i^o and y_i^m show observed and modelled values for i^{th} y , \bar{y}^o represents the average of observed values and N is the number of data points. Mean squared error (MSE) is the average of squared differences between modelled outcomes and observed values and is determined by $MSE = \frac{1}{N} \sum_{i=1}^N (y_i^o - y_i^m)^2$. In the case of the noisy data or when the data are not reliable, MSE can either overestimate or underestimate the badness of the prediction. Root mean squared error (RMSE), which is the squared root of MSE, usually shows better insight of the badness of the model. Normalised RMSE is used to evaluate the performance of the hybrid models in this study. $RMSE = \sqrt{\frac{1}{N} \sum_{i=1}^N (y_i^o - y_i^m)^2}$. Another measure for problems dealing with regression analysis is variance accounted for (VAF). VAF used the variance between the observed values and modelled values and is calculated as $VAF = \left[1 - \frac{\text{var}(y_i^o - y_i^m)}{\text{var}(y_i^o)} \right] \times 100$.

Results and discussions

Three hybrid evolutionary computational frameworks are developed to model the nonlinear relationships between the UCS of unsaturated cemented soil and its influential variables including cement content, dry

density, and suction. In this section, first the results of a parametric analysis, which is conducted to determine the optimum values of the parameters in each evolutionary algorithm, is illustrated. Then the results of the hybrid models are demonstrated on training and testing datasets. Lastly, a discussion is conducted based on the statistical analysis.

Result of parametric analysis

Hybridisation with evolutionary algorithms is executed to maximise the predictability level and minimise the error of ANN (see Fig. 4). Appropriate process optimisation requires for correctly selected parameters of algorithms using either parametric analysis or previous studies. In this paper, the parameters which are determined using previous studies are mentioned in the methodology description of the algorithms through Sections 3.21 to 3.3. In this section, the rest of the parameters are set using parametric investigations. In parametric analysis, optimum values of parameters are ascertained through RMSE analysis of the different values of the parameter using the hybrid algorithm (see Fig. 8). For ICA model, number of countries (N_{cou}) and number of imperialist (N_{imp}) are determined using RMSE analysis with the optimum values of 100 and 30, respectively (see Fig. 8 (a) and (b)). Fig. 8 (c) shows the RMSE analysis for number of chromosomes (N_{pop}) in GA model which depicts the optimum value of 150. Parametric investigation for number of particles (N_{pop}) in PSO model is illustrated in Fig. 8 (d) which shows the optimum value of 200. It is notable that number of decays (N_{dec}), the number of generations (N_{gen}) and the number of iteration (N_{itr}) which depict number of iterations for ICA, GA and PSO respectively, are determined using trial and error strategy. The parameters of models and their optimum values obtained in this study are shown in Table 2.

Training performance

Three hybrid evolutionary computational methods explained in previous section are used to predict the UCS of unsaturated cemented soils (see Fig. 9). The training dataset containing 67 cases is first used to train the model. Obtained results from the regression plots (left side) reveal that the PSO-ANN model achieved the highest R-squared value of

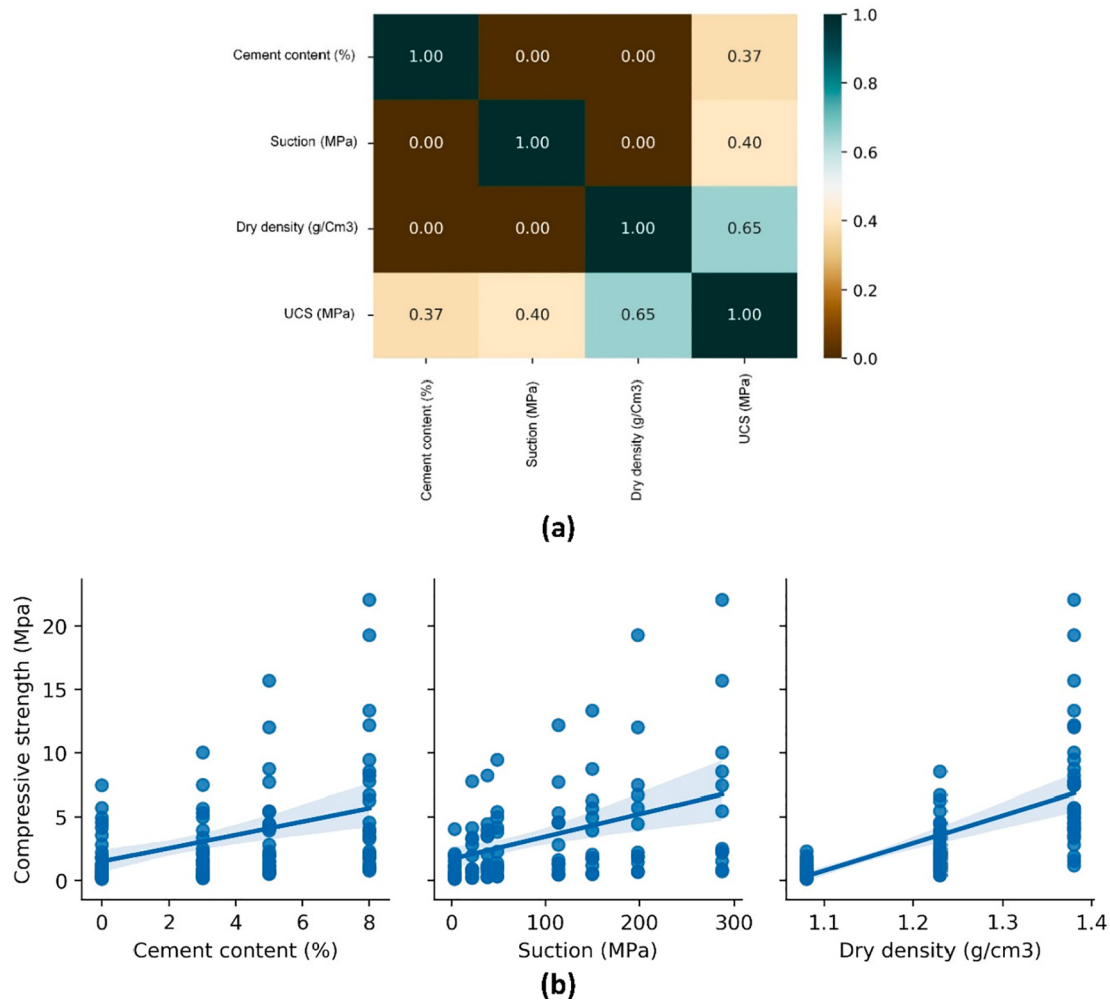


Fig. 5. (a) Correlation matrix and (b) relationships between input and output variables.

0.988, showing a great agreement between the predicted and measured values of the UCS. This value for GA-ANN and ICA-ANN is approximately the same with 0.9886 and 0.9828, respectively. It reveals that all the models show outstanding predictive performance. The right-hand side of the Fig. 9, which illustrates a comparison between predicted UCS values obtained from the models and measured UCS values for the training dataset, reveals that proposed models can successfully describe the nonlinear relationship between UCS and the influential parameters. It should be noted that, proposed models have better performance in predicting UCS lower than 15 (MPa). However, the predictive performance of the developed models for the UCS greater than 15 (MPa) is also very good.

Testing performance

The testing dataset (see Fig. 10) which contains the unseen data, i.e., the part of dataset on which no training process is conducted, is used as a validation phase to validate the performance of the proposed models which have been trained in the previous section. The regression plots (left side) show the R-squared value of 0.9412 for PSO-ANN which is the highest among three models. This is followed by GA-ANN ($R^2 = 0.921$) and ICA-ANN ($R^2 = 0.9014$) which shows the great agreement of the predicted values of the model and measured values of the experiments. The right-side plots in Fig. 10 shows the ability of the proposed models to mimic the unseen nonlinear relations.

Visualisation interpretation of result

Taylor diagram

As a mathematical visualisation technique which is designed to illustrate the accuracy of various models in the most suitable and compact way, Taylor diagram [62] is a concise summary of a statistical analysis that shows how well the results match the actual and developed models. In order to calculate the degree of (dis) similarity between the modelled results and the actual findings, this diagram appears to be a promising technique. A single point in this graph represents the correlation coefficient, the root-mean-square-difference, and the ratio of the two variables' standard deviations. The point closer to the 'reference point' indicates the ideal predictive model. Fig. 11 shows the Taylor diagrams for the developed models in the training and testing stages, indicating the positions of all the models by points (different markers). Position of the PSO-ANN appears to be closer to the 'reference point' which indicate this model as the best one.

Regression error characteristic curve

Regression error characteristic (REC) curve [63,64] in which the x-axis shows the error tolerance and y-axis depicts the precision of regression, is a variant of the receiver operating characteristic (ROC) curve in regression analysis. The error on the x-axis is generally described as a square error (SE) or absolute deviation (AD). However, the final curve determines the 'cumulative distribution function' of error, such as cdf. The curve which stands closer to the upper left corner indicates the more accurate model. To calculate the overall accuracy of

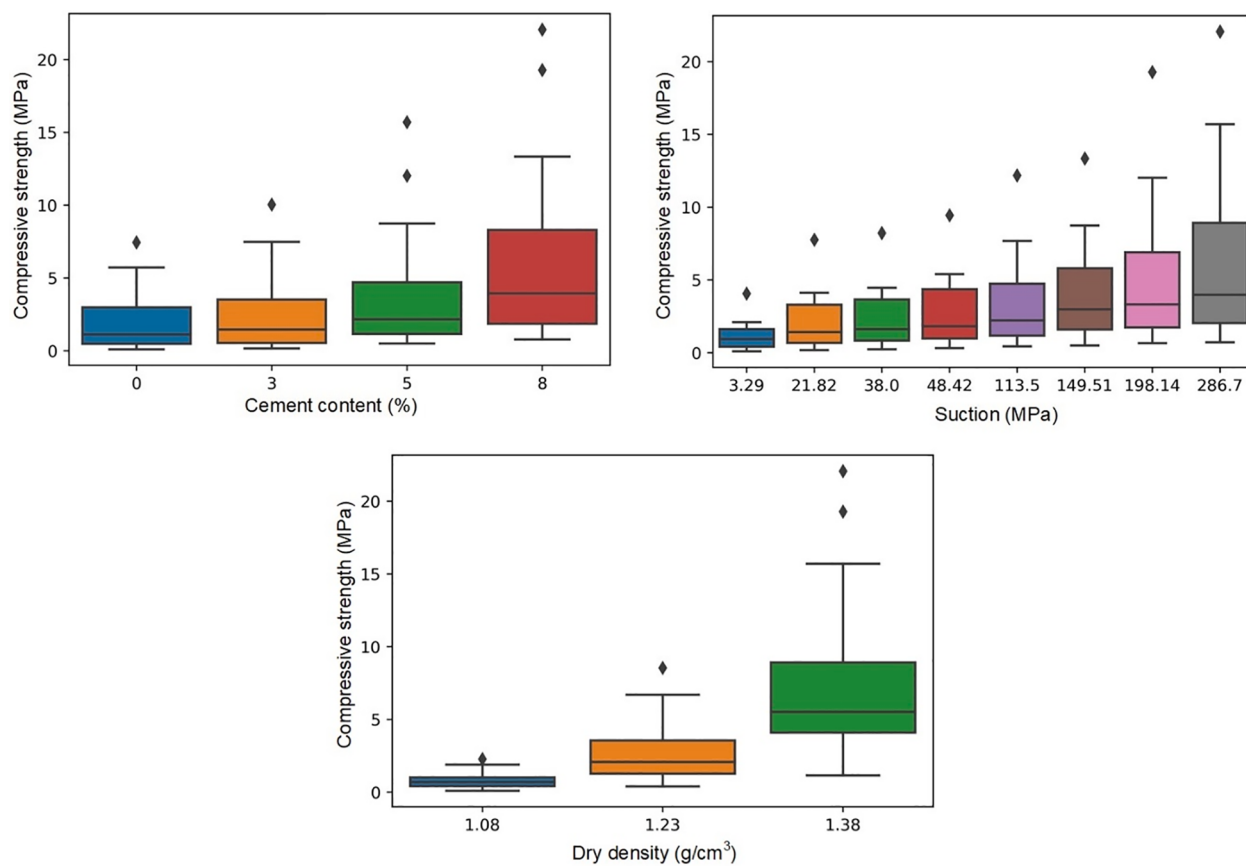


Fig. 6. Boxplots distributions of input variables.

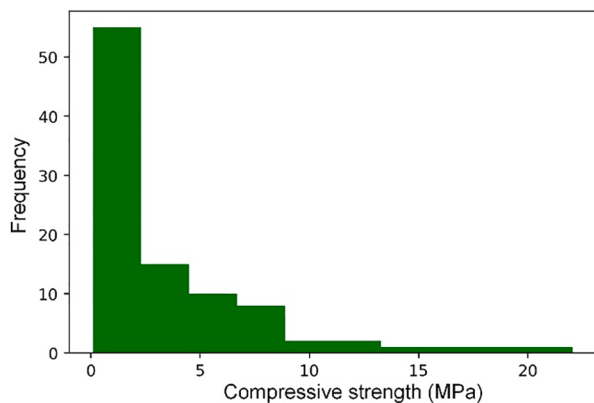


Fig. 7. Histogram distribution of the output variable.

the model, the value of the area under the curve (AUC) is measured and it should preferably be as large as possible to provide a proper prediction. This concept of error tolerance is extremely appealing because, because of uncertainties and errors in experiments, the probability of inaccuracy in most regression data is high. Fig. 12 illustrates the REC plots for three hybrid evolutionary approaches in the training and testing stages. Additionally, the AUC values have been shown in the figure. As can be seen, the highest AUC values in both training and testing stages have been achieved by PSO-ANN model with the $AUC = 0.9741$ and $AUC = 0.9142$, respectively.

Discussions based on statistical analysis

The statistical parameters are investigated for the training and

testing samples of each model and the results are compared. It should be noted that in this section a multilayer perceptron artificial neural network (MLPANN) which is a mostly used type of ANNs is also applied on the dataset and the results are compared to three proposed algorithms. One of the most important drawbacks of the MLPANN is the overfitting problem which means that the generated results have poor generalisation ability. According to Table 3, R^2 , RMSE and VAF values of models are approximately equal to one, zero and one. The R^2 , RMSE and VAF values for PSO-ANN (the weights and biases are listed in Appendix B) are 0.9888, 0.129, 97.742 for training dataset and 0.9412, 0.237, 90.414 for testing dataset. Therefore, in general, PSO-ANN performs better than the other two models. Using these statistical parameters along with the ranks system is employed to finalise the best model from these three models. The rank is calculated for each parameter for the training and testing samples of each model. Total rank in Table 3 shows the best model by final ranking which have lower rank score. Therefore, PSO-ANN, GA-ANN, ICA-ANN and MLPANN obtained the rank score of 7, 11, 18 and 24 respectively, which identified them as the best, better and good models based on statistical parameters performance rank of the model.

PSO-ANN which has been identified as the best model, is used to be compared with the experimental results. According to above analysis, PSO-ANN is successful to capture the nonlinear relations between UCS and its influential variables of different ranges.

Further investigation is conducted to reveal the relative importance (RI) score of the influential variables of the models using Gini importance analysis. The Gini importance, also known as the Mean Decrease in Impurity (MDI), determines the importance of each characteristic as the sum of the number of splits that include the feature, proportionate to the number of samples divided. The improvement in the split-criterion at each split in each tree is the important measure attributed to the splitting variable, and it is accumulated independently for each variable across all

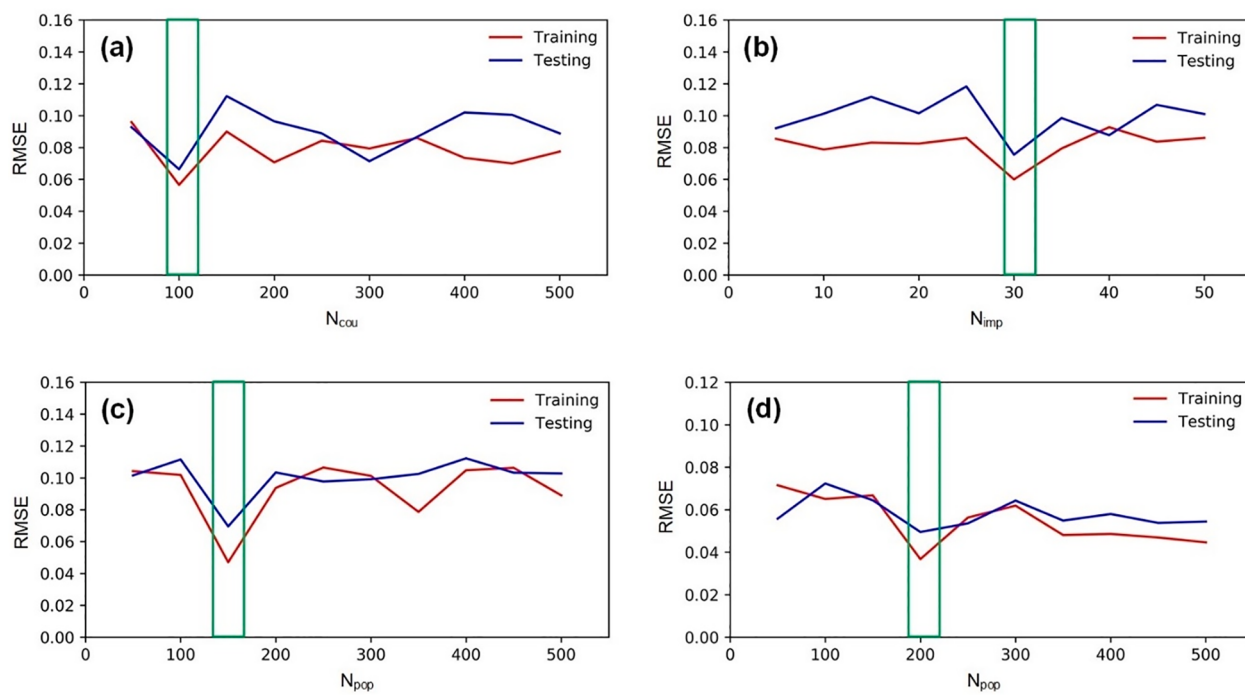


Fig. 8. Identifying the optimum parameters (a) GA: N_{cou} (b) PSO: N_{pop} (c) ICA: N_{cou} (d) ICA: N_{imp} .

Table 2
Optimum values of the parameters of algorithms.

Models	Parameter	Description	Range	Optimum value
ICA	N_{cou}	Number of Countries	50–500	100
	N_{imp}	Number of imperialists	5–50	30
GA	N_{dec}	Maximum number of decays	10–300	150
	N_{pop}	Number of chromosomes	50–500	150
PSO	N_{gen}	Maximum number of generations	10–300	150
	N_{pop}	Number of particles	50–500	200
	N_{itr}	Maximum number of iterations	10–300	200

the trees in the forest. A useful measure to quantify and evaluate relevant factors is a relative importance (RI) score based on Gini importance. According to Fig. 13, dry density has the highest RI score with the value of 59.8. This is followed by suction (RI = 23.3) and cement content (RI = 16.9).

Engineering database for unsaturated cemented Wenzhou clay

In this section, an engineering database is generated by using the developed PSO-ANN for different range of input variables including cement content from 1 to 11 (%) with the intervals of 1, suction from 1 to 300 (MPa) with the intervals of 10 and dry density from 1 to 1.5 (g/cm^3) with the intervals of 0.05. Hence, the dimension of the data would be $11 \times 31 \times 11$ which is equal to 3751 cases of unsaturated cemented Wenzhou clay. Subfigures in Fig. 14 illustrate the contour plots of the cases with different dry densities. In each subfigure, x-axis denotes the suction and y-axis is the cement content while coloured bands show the UCS ranges. Each subfigure features constant dry density. One hand, the engineering database shown in Fig. 14 can be directly used by engineers to estimate the UCS from a given dry density, cement content and suction that can be estimated by relative humidity (RH) roughly. On the other hand, Fig. 14 can also help engineers to design a suitable dosage of cement and determine optimal dry density for a targeted UCS under given environmental suctions.

Conclusion

In this study, three hybrid evolutionary models including GA-ANN, PSO-ANN and ICA-ANN have been developed to indicate the best model for predicting the unconfined compressive strength of unsaturated cemented soils. A dataset comprising of 96 cases is employed for the algorithms. The input variables for the proposed models include cement content, dry density and suction, while the output was UCS. Dataset was divided into training dataset, i.e., the part of dataset on which models are applied to learn the relationships between input and output variables with 70% of the cases (67 examples) and testing dataset, i.e., the part of the dataset which is considered as a validation phase of the modelling process, with 30% of the cases (29 examples). R-squared value (R^2), root mean square value (RMSE) and variance accounted for (VAF) are used as the performance metrics. First a parametric analysis was conducted to identify the optimum parameters of the optimisation algorithms which were hybridised with the artificial neural network (ANN). The topology of the ANN and some of the parameters of algorithms were determined using trial and error process against transition in RMSE value. Obtained results from the models revealed that proposed models have a good agreement with the experimental results, showing that hybrid evolutionary models can be used for predicting the UCS of unsaturated soils. The results also indicated that PSO-ANN achieved the highest rank regarding prediction of the UCS. The developed PSO-ANN can be used to generate engineering database for UCS which can facilitate the geotechnical design related to unsaturated cemented soils.

CRediT authorship contribution statement

Navid Kardani: Methodology, Investigation, Data curation, Validation, Writing - original draft. **Annan Zhou:** Conceptualization, Methodology, Investigation, Supervision, Writing - review & editing. **Shui-Long Shen:** Investigation, Supervision, Writing - review & editing. **Majidreza Nazem:** Investigation, Supervision, Writing - review & editing.

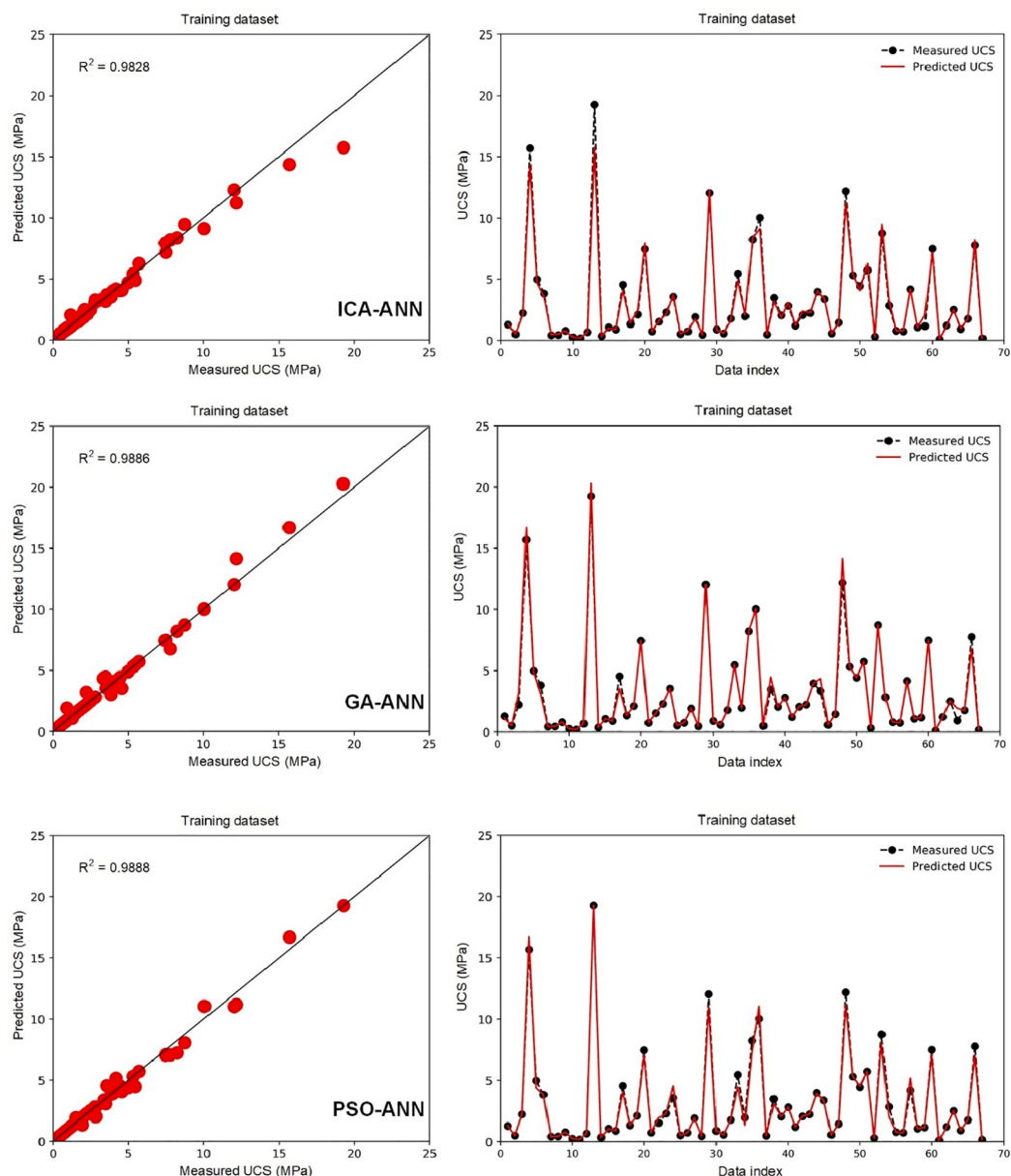


Fig. 9. Regression analysis of the models on the training dataset.

Declaration of Competing Interest

The authors declare that they have no known competing financial

interests or personal relationships that could have appeared to influence the work reported in this paper.

Appendix A

See Table A1.

Appendix B

The weights and biases of the PSO-ANN model are listed as follows.

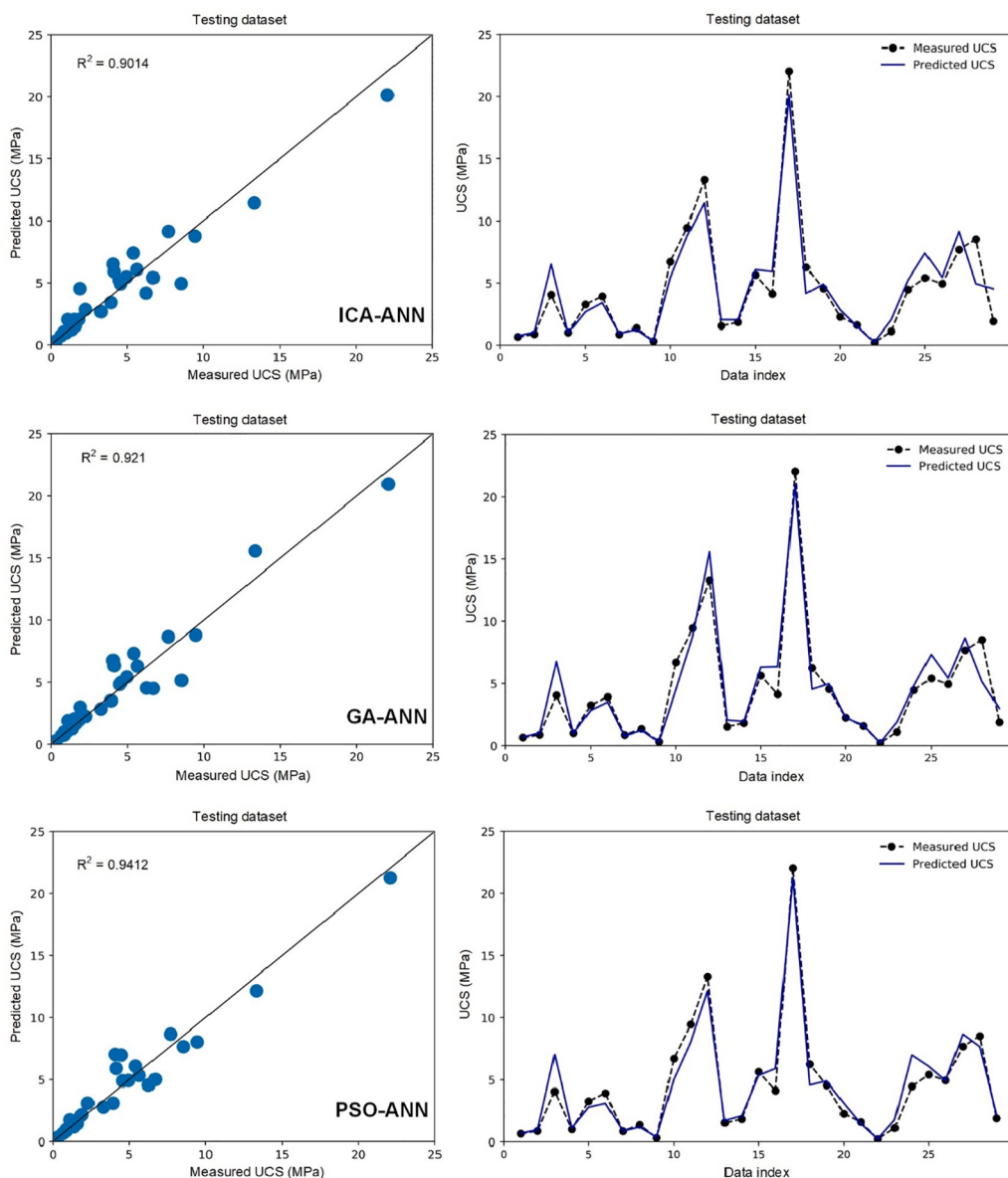


Fig. 10. Regression analysis of the models on the testing dataset.

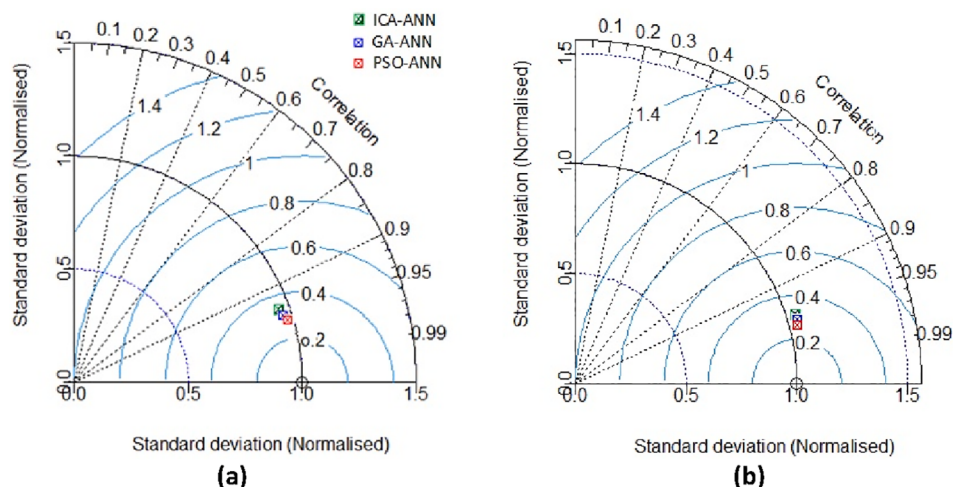


Fig. 11. Taylor diagrams of (a) training stage and (b) testing stage.

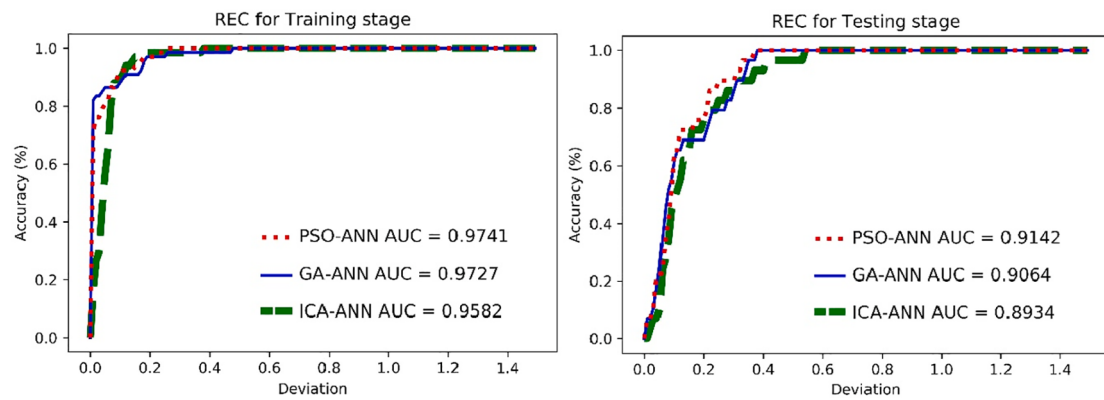


Fig. 12. REC curves of the hybrid models at training and testing stages.

Table 3
Statistical parameters of the proposed models.

Method		R ²	RMSE	VAF	Rank for R ²	Rank for RMSE	Rank for VAF	Total Rank
ICA-ANN	Training	0.9828	0.171	84.765	3	3	3	9
	Testing	0.9014	0.3	81.202	3	3	3	9
GA-ANN	Training	0.9886	0.136	92.004	2	2	2	6
	Testing	0.921	0.282	98.561	2	2	1	5
PSO-ANN	Training	0.9888	0.129	97.742	1	1	1	3
	Testing	0.9412	0.237	90.414	1	1	2	4
MLPANN	Training	0.9623	0.191	91.231	4	4	4	12
	Testing	0.8482	0.364	80.514	4	4	4	12

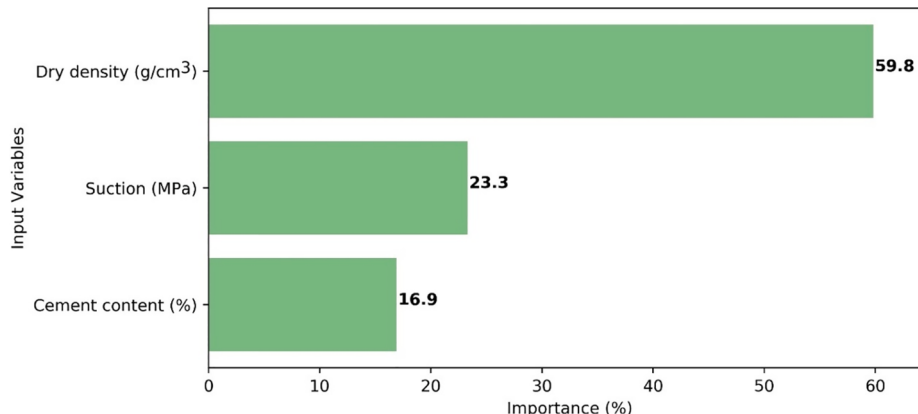


Fig. 13. Variable importance analysis of the input variables.

$$\mathbf{IW} = \begin{pmatrix} -19.9024 & 10.0474 & -18.3421 \\ -13.2901 & -12.7450 & -10.4697 \\ 0.0084 & 2.3274 & 4.8063 \\ -17.0523 & 34.9449 & -57.3870 \\ -0.0848 & 28.7694 & 46.2872 \\ 0.0103 & -0.2261 & 7.6668 \\ -1.5944 & -0.2911 & 0.1854 \\ 1.4138 & 0.2512 & -0.1780 \\ 0.0003 & 2.3122 & -2.6337 \\ -0.0388 & 0.8276 & -2.0877 \end{pmatrix}$$

$$\mathbf{LW} = \{0.0875, -15.3063, -26.7280, -0.1435, 3.4339, 28.1151, 12.0544, 13.4517, 27.1652, 4.2146\}$$

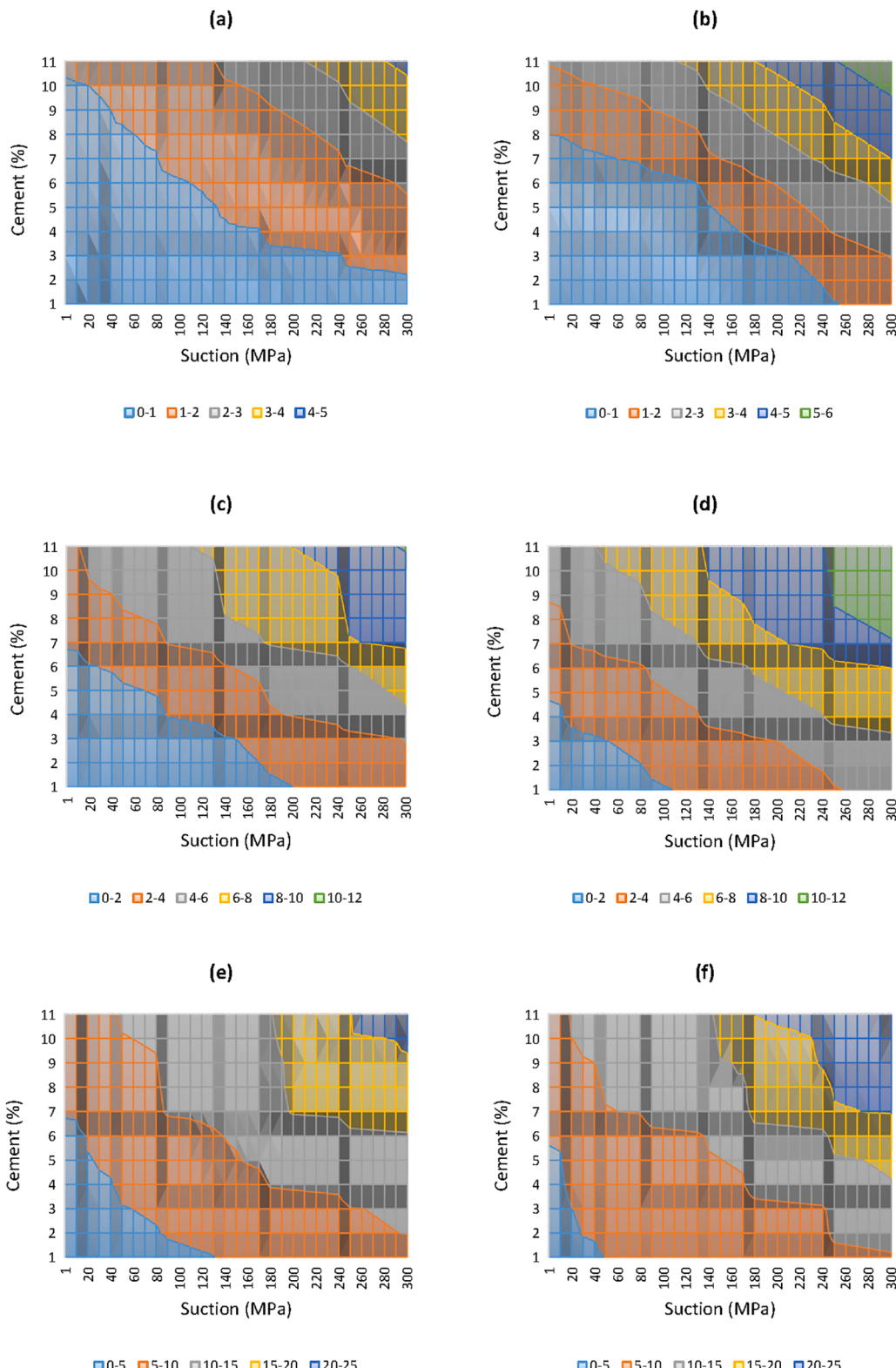


Fig. 14. Contour plots for UCS modelling using PSO-ANN: a) dry density = 1 (g/cm^3), b) dry density = 1.1 (g/cm^3), c) dry density = 1.2 (g/cm^3), d) dry density = 1.3 (g/cm^3), e) dry density = 1.4 (g/cm^3) and f) dry density = 1.5 (g/cm^3).

Table A1

The dataset used in the study (data extracted from [3]).

Cement content (%)	Suction (MPa)	Dry density (g/cm ³)	UCS (MPa)	Cement content (%)	Suction (MPa)	Dry density (g/cm ³)	UCS (MPa)
0	3.29	1.38	1.16	0	113.5	1.38	4.55
3	3.29	1.38	1.54	3	113.5	1.38	5.31
5	3.29	1.38	1.91	5	113.5	1.38	7.68
8	3.29	1.38	4.06	8	113.5	1.38	12.2
0	3.29	1.23	0.41	0	113.5	1.23	1.32
3	3.29	1.23	0.43	3	113.5	1.23	1.60
5	3.29	1.23	1.10	5	113.5	1.23	2.82
8	3.29	1.23	2.11	8	113.5	1.23	4.55
0	3.29	1.08	0.10	0	113.5	1.08	0.45
3	3.29	1.08	0.17	3	113.5	1.08	0.48
5	3.29	1.08	0.51	5	113.5	1.08	0.87
8	3.29	1.08	0.78	8	113.5	1.08	1.28
0	21.82	1.38	2.80	0	149.51	1.38	4.94
3	21.82	1.38	3.36	3	149.51	1.38	5.65
5	21.82	1.38	4.12	5	149.51	1.38	8.74
8	21.82	1.38	7.77	8	149.51	1.38	13.3
0	21.82	1.23	0.72	0	149.51	1.23	1.75
3	21.82	1.23	0.88	3	149.51	1.23	2.03
5	21.82	1.23	1.95	5	149.51	1.23	3.93
8	21.82	1.23	3.28	8	149.51	1.23	6.26
0	21.82	1.08	0.18	0	149.51	1.08	0.50
3	21.82	1.08	0.22	3	149.51	1.08	0.56
5	21.82	1.08	0.56	5	149.51	1.08	1.19
8	21.82	1.08	0.88	8	149.51	1.08	1.76
0	38	1.38	3.55	0	198.14	1.38	5.72
3	38	1.38	3.97	3	198.14	1.38	7.48
5	38	1.38	4.46	5	198.14	1.38	12.0
8	38	1.38	8.22	8	198.14	1.38	19.3
0	38	1.23	0.91	0	198.14	1.23	1.83
3	38	1.23	1.20	3	198.14	1.23	2.22
5	38	1.23	2.06	5	198.14	1.23	4.44
8	38	1.23	3.47	8	198.14	1.23	6.70
0	38	1.08	0.24	0	198.14	1.08	0.66
3	38	1.08	0.29	3	198.14	1.08	0.73
5	38	1.08	0.65	5	198.14	1.08	1.44
8	38	1.08	1.00	8	198.14	1.08	1.90
0	48.42	1.38	4.16	0	286.7	1.38	7.44
3	48.42	1.38	4.98	3	286.7	1.38	10.0
5	48.42	1.38	5.41	5	286.7	1.38	15.7
8	48.42	1.38	9.44	8	286.7	1.38	22.1
0	48.42	1.23	1.06	0	286.7	1.23	2.21
3	48.42	1.23	1.37	3	286.7	1.23	2.50
5	48.42	1.23	2.27	5	286.7	1.23	5.46
8	48.42	1.23	3.83	8	286.7	1.23	8.53
0	48.42	1.08	0.32	0	286.7	1.08	0.72
3	48.42	1.08	0.35	3	286.7	1.08	0.87
5	48.42	1.08	0.78	5	286.7	1.08	1.52
8	48.42	1.08	1.05	8	286.7	1.08	2.29

$$\mathbf{b1} = \begin{pmatrix} 22.0394 \\ 30.4652 \\ -3.2012 \\ -30.4485 \\ -15.9330 \\ -1.0933 \\ -1.1822 \\ 1.0866 \\ 4.2392 \\ -0.2386 \end{pmatrix}$$

$$\mathbf{b2} = \{-13.6055\}$$

References

- [1] Bruno AW, Gallipoli D, Rouainia M, Lloret-Cabot M. A bounding surface mechanical model for unsaturated cemented soils under isotropic stresses. Comput Geotech 2020;125:103673.
- [2] Consoli NC, de Moraes RR, Festugato L. Parameters controlling tensile and compressive strength of fiber-reinforced cemented soil. J Mater Civ Eng 2013;25(10):1568–73.
- [3] Yu C, Wang H, Zhou A, Cai X, Wu Z. Experimental study on strength and microstructure of cemented soil with different suctions. J Mater Civ Eng 2019;31(6):04019082.
- [4] Bahar R, Benazzoug M, Kenai S. Performance of compacted cement-stabilised soil. Cem Conc Compos 2004;26(7):811–20.
- [5] Consoli NC, Foppa D, Festugato L, Heineck KS. Key parameters for strength control of artificially cemented soils. J Geotech Geoenvir Eng 2007;133(2):197–205.

- [6] Bhattacharja S, Bhatty J. Comparative performance of portland cement and lime stabilization of moderate to high plasticity clay soils. *Portl Cem Assoc* 2003.
- [7] Horpibulsuk S, Miura N, Nagaraj T. Clay-water/cement ratio identity for cement admixed soft clays. *J Geotech Geoenviron Eng* 2005;131(2):187–92.
- [8] Yao Y, Zhou A. Non-isothermal unified hardening model: a thermo-elasto-plastic model for clays. *Geotechnique* 2013;63(15):1328–45.
- [9] Wu S, Zhou A, Li J, Kodikara J, Cheng W-C. Hydromechanical behaviour of overconsolidated unsaturated soil in undrained conditions. *Can Geotech J* 2019;56(11):1609–21.
- [10] Zhou A, Huang R, Sheng D. Capillary water retention curve and shear strength of unsaturated soils. *Can Geotech J* 2016;53(6):974–87.
- [11] Alavi AH, Gandomi AH, Sahab MG, Gandomi M. Multi expression programming: a new approach to formulation of soil classification. *Eng Comput* 2010;26(2):111–8.
- [12] Baziar M, Jafarian Y. Assessment of liquefaction triggering using strain energy concept and ANN model: capacity energy. *Soil Dyn Earthquake Eng* 2007;27(12):1056–72.
- [13] Javdanian H. Evaluation of soil liquefaction potential using energy approach: experimental and statistical investigation. *Bull Eng Geol Environ* 2019;78(3):1697–708.
- [14] Shen S-L, Njock PGA, Zhou A, Lyu H-M. Dynamic prediction of jet grouted column diameter in soft soil using Bi-LSTM deep learning. *Acta Geotech* 2020;1–13.
- [15] Jafarian Y, Haddad A, Javdanian H. Predictive model for normalized shear modulus of cohesive soils. *Training* 2014;132(575):6.
- [16] Gordian B, Armaghani DJ, Hajihassani M, Monjezi M. Prediction of seismic slope stability through combination of particle swarm optimization and neural network. *Eng Comput* 2016;32(1):85–97.
- [17] Kardani N, Zhou A, Nazem M, Shen S-L. Improved prediction of slope stability using a hybrid stacking ensemble method based on finite element analysis and field data. *J Rock Mech Geotech Eng* 2020.
- [18] Kardani N, Zhou A, Nazem M, Shen S-L. Estimation of bearing capacity of piles in cohesionless soil using optimised machine learning approaches. *Geotech Geol Eng* 2019;1–21.
- [19] Samui P. Determination of ultimate capacity of driven piles in cohesionless soil: a multivariate adaptive regression spline approach. *Int J Numer Anal Meth Geomech* 2012;36(11):1434–9.
- [20] Javdanian H, Lee S. Evaluating unconfined compressive strength of cohesive soils stabilized with geopolymers: a computational intelligence approach. *Eng Comput* 2019;35(1):191–9.
- [21] Das SK, Samui P, Sabat AK. Application of artificial intelligence to maximum dry density and unconfined compressive strength of cement stabilized soil. *Geotech Geol Eng* 2011;29(3):329–42.
- [22] Ghorbani A, Hasanzadehshoaili H. Prediction of UCS and CBR of microsilica-lime stabilized sulfate silty sand using ANN and EPR models; application to the deep soil mixing. *Soils Found* 2018;58(1):34–49.
- [23] Mahmoodzadeh A, Mohammadi M, Ibrahim HH, Abdulhamid SN, Salim SG, Ali HFH, et al. Artificial intelligence forecasting models of uniaxial compressive strength. *Transp Geotech* 2021;27:100499.
- [24] Pham BT, Nguyen MD, Nguyen-Thoi T, Ho LS, Koopalipoor M, Quoc NK, et al. A novel approach for classification of soils based on laboratory tests using Adaboost, Tree and ANN modeling. *Transp Geotech* 2020;100508.
- [25] Kardani MN, Baghban A, Hamzehi ME, Baghban M. Phase behavior modeling of asphaltene precipitation utilizing RBF-ANN approach. *Pet Sci Technol* 2019;37(16):1861–7.
- [26] Momeni E, Yarivand A, Dowlatshahi MB, Armaghani DJ. An efficient optimal neural network based on Gravitational Search Algorithm in predicting the deformation of geogrid-reinforced soil structures. *Transp Geotech* 2021;26:100446.
- [27] Alzabeebee S, Chapman DN. Evolutionary computing to determine the skin friction capacity of piles embedded in clay and evaluation of the available analytical methods. *Transp Geotech* 2020;24:100372.
- [28] Kardani N, Zhou A, Nazem M, Lin X. Modelling of municipal solid waste gasification using an optimised ensemble soft computing model. *Fuel* 2021;289:119903.
- [29] Kardani N, Bardhan A, Kim D, Samui P, Zhou A. Modelling the energy performance of residential buildings using advanced computational frameworks based on RVM, GMDH, ANFIS-BBO and ANFIS-IPSO. *J Build Eng* 2021;35:102105.
- [30] Apostolopoulou M, Asteris PG, Armaghani DJ, Douvika MG, Lourenco PB, Cavalieri L, et al. Mapping and holistic design of natural hydraulic lime mortars. *Cem Concr Res* 2020;136:106167.
- [31] Asteris PG, Plevris V. Anisotropic masonry failure criterion using artificial neural networks. *Neural Comput Appl* 2017;28(8):2207–29.
- [32] Asteris PG, Moropoulou A, Skentou AD, Apostolopoulou M, Mohebbkhah A, Cavalieri L, et al. Stochastic vulnerability assessment of masonry structures: concepts, modeling and restoration aspects. *Appl Sci* 2019;9(2):243.
- [33] Zhang P, Yin Z-Y, Jin Y-F. State-of-the-art review of machine learning applications in constitutive modeling of soils. *Arch Comput Methods Eng* 2021;1–26.
- [34] Zhang P, Yin Z-Y, Jin Y-F, Chan TH, Gao F-P. Intelligent modelling of clay compressibility using hybrid meta-heuristic and machine learning algorithms. *Geosci Front* 2021;12(1):441–52.
- [35] Zhang P, Yin Z-Y, Jin Y-F, Chan TH. A novel hybrid surrogate intelligent model for creep index prediction based on particle swarm optimization and random forest. *Eng Geol* 2020;265:105328.
- [36] Yin ZY, Jin YF, Shen JS, Hicher PY. Optimization techniques for identifying soil parameters in geotechnical engineering: comparative study and enhancement. *Int J Numer Anal Meth Geomech* 2018;42(1):70–94.
- [37] Jin Y-F, Yin Z-Y, Shen S-L, Zhang D-M. A new hybrid real-coded genetic algorithm and its application to parameters identification of soils. *Inverse Prob Sci Eng* 2017;25(9):1343–66.
- [38] Jin Y-F, Yin Z-Y, Shen S-L, Hicher P-Y. Investigation into MOGA for identifying parameters of a critical-state-based sand model and parameters correlation by factor analysis. *Acta Geotech* 2016;11(5):1131–45.
- [39] Jin YF, Yin ZY. Enhancement of backtracking search algorithm for identifying soil parameters. *Int J Numer Anal Meth Geomech* 2020;44(9):1239–61.
- [40] Atashpaz-Gargari E, Lucas C. Imperialist competitive algorithm: an algorithm for optimization inspired by imperialistic competition. In: 2007 IEEE congress on evolutionary computation. IEEE; 2007:4661–7.
- [41] Kaveh A, Talatahari S. Optimum design of skeletal structures using imperialist competitive algorithm. *Comput Struct* 2010;88(21–22):1220–9.
- [42] Khabbazi A, Atashpaz-Gargari E, Lucas C. Imperialist competitive algorithm for minimum bit error rate beamforming. *Int J Bio-Inspired Comput* 2009;1(1–2):125–33.
- [43] Holland John H. Genetic algorithms. *Sci Am* 1992;267(1):44–50.
- [44] Mühlénbein H, Schomisch M, Born J. The parallel genetic algorithm as function optimizer. *Parallel Comput* 1991;17(6–7):619–32.
- [45] Levasseur S, Malécot Y, Boulon M, Flavigny E. Soil parameter identification using a genetic algorithm. *Int J Numer Anal Meth Geomech* 2008;32(2):189–213.
- [46] Schmitt LM. Theory of genetic algorithms. *Theoret Comput Sci* 2001;259(1–2):1–61.
- [47] Eberhart R, Kennedy J. A new optimizer using particle swarm theory. In: MHS'95. Proceedings of the Sixth International Symposium on Micro Machine and Human Science. IEEE; 1995:39–43.
- [48] Baghban A, Kardani MN, Mohammadi AH. Improved estimation of Cetane number of fatty acid methyl esters (FAMEs) based biodiesels using TLBO-NN and PSO-NN models. *Fuel* 2018;232:620–31.
- [49] Kennedy J, Eberhart R. Particle swarm optimization. In: Proceedings of ICNN'95-International Conference on Neural Networks. 4. IEEE; 1995:1942–8.
- [50] Kardani MN, Baghban A, Sasanipour J, Mohammadi AH, Habibzadeh S. Group contribution methods for estimating CO₂ absorption capacities of imidazolium and ammonium-based polyionic liquids. *J Cleaner Prod* 2018;203:601–18.
- [51] Ghambri A, Kardani MN, Moazami Goodarzi A, Janghorban Larieh M, Baghban A. Neural computing approach for estimation of natural gas dew point temperature in glycol dehydration plant. *Int J Ambient Energy* 2020;41(7):775–82.
- [52] Kardani MN, Baghban A. Utilization of LSSVM strategy to predict water content of sweet natural gas. *Pet Sci Technol* 2017;35(8):761–7.
- [53] Khandelwal M, Mahdiyar A, Armaghani DJ, Singh T, Fahimifar A, Faradonbeh RS. An expert system based on hybrid ICA-ANN technique to estimate macerals contents of Indian coals. *Environ Earth Sci* 2017;76(11):399.
- [54] Moayedi H, Armaghani DJ. Optimizing an ANN model with ICA for estimating bearing capacity of driven pile in cohesionless soil. *Eng Comput* 2018;34(2):347–56.
- [55] Tian H, Shu J, Han L. The effect of ICA and PSO on ANN results in approximating elasticity modulus of rock material. *Eng Comput* 2019;35(1):305–14.
- [56] Chandwani V, Agrawal V, Nagar R. Modeling slump of ready mix concrete using genetic algorithms assisted training of Artificial Neural Networks. *Expert Syst Appl* 2015;42(2):885–93.
- [57] Taghavi M, Gharehghani A, Nejad FB, Mirsalim M. Developing a model to predict the start of combustion in HCCI engine using ANN-GA approach. *Energy Convers Manage* 2019;195:57–69.
- [58] Yuce B, Rezgui Y, Mourshed M. ANN-GA smart appliance scheduling for optimised energy management in the domestic sector. *Energy Build* 2016;111:311–25.
- [59] da Silva Veloso YM, de Almeida MM, de Alencastro OLS, Passos ML, Mujumdar AS, Leite MS. Hybrid phenomenological/ANN-PSO modelling of a deformable material in spouted bed drying process. *Powder Technol* 2020;366:185–96.
- [60] Khatir S, Tiachacht S, Thanh C-L, Bui TQ, Wahab MA. Damage assessment in composite laminates using ANN-PSO-IGA and Cornwell indicator. *Compos Struct* 2019;230:111509.
- [61] Vasumathi B, Moorthi S. Implementation of hybrid ANN-PSO algorithm on FPGA for harmonic estimation. *Eng Appl Artif Intell* 2012;25(3):476–83.
- [62] Taylor KE. Summarizing multiple aspects of model performance in a single diagram. *J Geophys Res: Atmos* 2001;106(D7):7183–92.
- [63] Bi J, Bennett KP. Regression error characteristic curves. In: Proceedings of the 20th international conference on machine learning (ICML-03). 2003:43–50.
- [64] Kardani N, Bardhan A, Samui P, Nazem M, Zhou A, Armaghani DJ. A novel technique based on the improved firefly algorithm coupled with extreme learning machine (ELM-IFF) for predicting the thermal conductivity of soil. *Eng Comput* 2021;1–20.